Aging of polyamide 11. Part 1: Evaluating degradation by thermal, mechanical, and viscometric analysis

Tobiasz Mazan,[1] Randi Berggren,[1] Jens Kjær Jørgensen,[2] Andreas Echtermeyer[1]

[1]Department of Engineering Design and Materials, Norwegian University of Science and Technology, Trondheim 7034, Norway
[2]SINTEF Materials and Chemistry, Oslo 0373, Norway
Correspondence to: T. Mazan (E-mail: tobiasz.mazan@ntnu.no)

ABSTRACT: Hydrolytic degradation at elevated temperatures is a key reason for failure in offshore flexible risers. In this article, the aging of polyamide 11 in deoxygenated water at 90°C and 120°C was studied. Tensile and dynamic mechanical thermal analysis tests were performed to measure changes in mechanical properties. Viscometry, gravimetric measurements, differential scanning calorimetry, and thermogravimetric analysis were used to link these properties with morphological changes. General trends are increased stiffness, tensile strength, and glass transition temperature as well as decreased glassy state damping efficiency with increased aging times. Changes can be initially ascribed to plasticizer depletion and then to interplay between molecular weight decrease and crystallinity increase. Viscosity at hydrolysis equilibrium indicates that brittle failure typically involves oxidation or UV exposure. © 2015 Wiley Periodicals, Inc. J. Appl. Polym. Sci. 2015, 132, 41971.

INTRODUCTION

Polyamides PA are known to undergo chemical degradation if they are exposed to oil and gas field exploration environments. The degradation leads to loss of mechanical properties and subsequently affects the lifetime of the given structure.[1]

A very important application for PA is flexible risers. Oilfield flexible risers convey high temperature production fluids (typically mixtures of oil, gas, and water) from subsea units on the seabed to topside platforms. The risers are multilayered pipes of metal and polymers designed to have high axial stiffness and rather low bending stiffness. They have an internal polymer sheath to keep the transported fluid inside the pipe. Unbounded metal strips are wound around this sheath (in so called annulus) to provide strength and stiffness. An outer thermoplastic sheath is a barrier against seawater ingress. More details and drawing can be found in API 17B.[2]

The offshore environment presents many structural challenges to the flexible risers, such as the fluctuating dynamic loads imposed by surface waves and underwater currents. The polymer sheaths do not provide any structural strength, but they need to follow all deformations of the structure over its entire life. This means they need a fairly high strain to failure (a few %) and good fracture toughness. Strength and stiffness of the polymer sheath are needed to bridge the gaps between the metal parts and to prevent excessive creep into the gaps.

Polyamide 11 (PA11) is one of the most common materials used for the internal pressure sheaths in flexible risers due to good fatigue and creep resistance as well as decent barrier properties toward oil and natural gas.[3] Among the production fluids crude oil and gas cause mainly swelling of the polymer, therefore the transported high temperature water is a primary reason for degradation of PA11 internal pressure sheath. The structural integrity of this element is of great importance for environmental, economical and safety reasons. Nevertheless, almost 20% of the flexible pipe failure incidents in United Kingdom and Norway are related to aged internal sheaths.[4]

Industry and academic research have given aging of polyamides much attention over the past decades. Numerous aging experiments have been conducted on polyamides in different environments. Most studies used the decreasing molecular weight of the polymer chains as an indicative property of aging that can be related to the fracture toughness or failure strain of the material.[1,5] Much effort has also been put into creating

degradation models based on hydrolysis, which is established as the governing chain scission mechanism for PA11 in water at elevated temperatures.[6,7] Still, the aging process of polyamides is complex and looking at the molecular weight reduction alone does not give an adequate overview of the material degradation. In addition to chain scission due to chemical reactions there are structural changes from annealing upon heating and chemicrystalization, as well as swelling by water uptake and plasticizer loss. These two last processes cause structural changes that are not detectable by molecular weight measurements, but may drastically affect the mechanical properties of the polyamide. Some investigations go a step further reporting additional morphological parameters and final properties such as degree of crystallinity,[8,9] glass transition temperature,[10] modulus,[10,11] or plasticizer content.[9–11] None of them however treat all these effects simultaneously and they don't consider additional quantities reported in this work such as density, water uptake, tangential modulus, tensile strength, and damping efficiency. The correlation between aging and changes in mechanical properties for PA11 is thus neither extensively described nor understood.

The purpose of this work was to investigate in detail the mechanical and volumetric properties of PA11 during degradation as well as the correlation between them and key morphological parameters. Accelerated aging tests were performed in oxygen depleted water at 90°C and 120°C. Contrary to many of the previous publications[9–11] full evolution of each property up to 10 weeks of aging was reported, which is of particular importance for comparing experiments with degradation model predictions—the second part of our "Aging of Polyamide 11" study.[12]

EXPERIMENTAL

In this work the aging process of PA11 was examined by tracking the changes in mechanical properties. The mechanical test methods in question were tensile testing and dynamic mechanical thermal analysis (DMTA). The latter was performed to follow changes in the glass transition temperature and storage modulus. Weight measurements were performed to keep track on sample density and weight loss. Thermal gravimetric analysis investigated plasticizer extraction and differential scanning calorimetry (DSC) crystallinity evolution.

Material

The PA11 under study was Rilsan® BESNO TL40 from Arkema, which is widely used for offshore applications. The Arkema product specification states that this is an extrusion or blow molded PA11 with normal viscosity, no color additives, medium flexibility and added heat and light stabilizers.[3] The material contains nominally 12.5% N-butyl-benzenesulfonamide (BBSA) plasticizer.

Specimen Preparation.

The samples were cut from an unused circular pressure sheath made for a flexible riser. Strips with a thickness of approximate 0.5 mm were cut from the pressure sheath in a manner so that the cross-section of the pressure sheath constituted the width of the strips. Thin specimens were used to bring out the effects of plasticizer loss and water penetration quickly. Moreover both aging and plasticizer content

becomes more homogenous for thin sheet samples. Specimens for tensile testing and dynamic mechanical analysis were punched or cut from the strips after exposure since the thin samples tend to deform during aging. This procedure ensured an uniform sample geometry for the mechanical tests. For material aged 3 weeks or more surface cracks were observed on the dumbbells for tensile testing. These cracks were initiated when the samples were punched out from the strips. The cracks could potentially reduce the strength of a brittle material, however we have assumed their effect is negligible in the case of ductile material. This study also focused more on the shape of the stress vs. strain curve than the absolute strength, making crack development not so critical.

Accelerated Aging

Internal pressure sheath PA11 in operative risers is exposed to an oxygen free environment.[7] In order to perform experiments as close as possible to these conditions oxygen had to be removed from the accelerated aging environment. Testing in oxygen free water is also interesting from a theoretical point of view, because it allows studying aging due to H_2O without any influence from oxygen.

Samples analyzed with DSC were aged with initially developed procedure. In the initial procedure a thin sheet samples of 100 mg were cut out and placed in a 20-mL vial (Part no. 354833 from Biotage). Then 20 mL deionized water was added. The liquid to sample volume ratio was between 25 and 200. The liquid had been deoxygenated by bubbling through Argon 6.0 for 3 h and the vial was flushed with Argon before adding the liquid. The vials were sealed and placed in a heating oven at a designated temperature for a preset time, up to 32 days. The vials were only opened after completed aging. No discoloration of samples was observed indicating that deoxygenation was satisfactory. Nevertheless it was decided to improve the aging procedure for mechanical, gravimetric, and viscometric tests. The new procedure allowed for a better oxygen and temperature control in the process, but otherwise it introduced no major differences.

Aging of the PA11 samples with improved procedure was performed in a 17-L closed stainless steel 254 SMO autoclave. The thin sheet samples of 0.5 mm were thread onto a metal wire hanging from the lid of the autoclave ensuring exposure of the samples from both sides. The autoclave was filled with 15 L distilled water. To prevent oxidative degradation processes the water was deoxygenized to a level of 2–4 ppb oxygen by bubbling with nitrogen gas (N_2 5.0) for approximately 20 h. The autoclave was then placed on a plate heater and heated up to 120°C as measured with a thermocouple inside the fluid chamber. The autoclave was opened for sample retrieval every week the first month, then every second week up to 10 weeks. The oxygen content of the water at the end of each exposure period was measured with a Hach Orbisphere 410 sensor, which revealed no major changes. Every time the autoclave was opened the water was replaced and the nitrogen-bubbling routine repeated before the heat was turned on again.

Choice of Aging Parameters.

The choice of times and temperatures for the aging tests in this study was based on the

hydrolytic degradation model proposed by Jacques.[7] Industry practice requires that the corrected inherent viscosity (CIV) does not drop below 1.2 dL/g.[1] As given by the Jacques relationship in eq. (2) the acceptance criteria corresponds to Mw of 34.7 kg/mol and should be reached after about 5 weeks in water at 120°C.[7] According to Jacques the molecular weight should drop further until it becomes stable after 7 weeks at 120°C. The aging was run up to 10 weeks to make sure the equilibrium was reached.

Material Storage and Handling

Density and DMTA measurements were performed on the aged (water saturated) samples the same day as they were withdrawn from the water bath. Due to difficulties with the equipment, samples for the other characterization methods were tested at a later time. To ensure that the aged material did not change before characterization the samples were put in distilled water in glass bottles and stored in a refrigerator. Some of the samples were placed in desiccator at room temperature 48 h prior to the tensile tests to remove moisture, others were tested in saturated state.

Material Analysis

Gravimetric Measurements. The density was found by Archimedes' principle. The mass of the samples in air and apparent mass upon immersion in water at 23°C was determined using an analytical balance with a sample holder.

The specific gravity and density was calculated as described in the ASTM D792-08 Standard Test Methods for Density and Specific Gravity (Relative Density) of Plastics by Displacement.[13]

Volatile Content. Fourier transform infrared spectroscopy (FTIR) measurements were performed for reference sample and one aged 20 days in 90°C. However, no significant change in spectra was observed and finally sample mass loss at elevated temperature was chosen as preferred method to determine amount of extractables. For samples aged in oxygen-containing water at 90°C the amount of volatile compounds was determined by thermogravimetric analysis (TGA) in a nitrogen atmosphere using a Pyris 1 TGA from PerkinElmer. Samples were heated at 5°C/min from 20°C to 310°C. The mass loss between 30°C and 110°C was attributed to water loss and the mass loss between 110°C and 310°C was attributed to loss of plasticiser. The latter one can be therefore thought of as the remaining content of plasticizer in the sample after specified exposure time. The volatile content for samples aged in oxygen-free water in 90°C and 120°C was determined by mass loss after 90 min in a vacuum oven at 200°C.

Corrected Inherent Viscosity. The inherent viscosity IV was determined based on the description from API 17TR2.[1] The PA11 was dissolved in *m*-cresol (C85727 99% solution from Sigma-Aldrich) to a concentration of 5.00 mg/cm³. The frequency dependent viscosity of the solution was measured using a plate-plate rheometer (Anton Paar MCR 300) in the frequency range 100–400 s⁻¹ and the average viscosity in this range is used to calculate the IV. The API 17TR2 specifies the use of a capillary rheometer for measuring the viscosity, but

a plate-plate rheometer was used here to provide better control of the shear rate and temperature. Since PA11 used in flexible risers contains additives the measured IV needs to be corrected in order to obtain viscosity of pure PA11. The CIV is given by[1]:

$$CIV = \frac{IV}{(1-\text{extrable content})} \qquad (1)$$

Present data consists of single measurements.

Relation Between CIV and Molecular Weight. The relation between measured CIV and weight-average molecular weight was calculated with Jacques empirical relationship similar to Mark-Houwink equation, however operating directly on M_w and not on viscosity-average molecular weight:

$$CIV = 10^{(0.58121 \times \log(M_w) - 2.5595)} \qquad (2)$$

where M_w is the weight-average molecular weight.[7] The number average molecular weight M_n can be calculated with the formula:

$$M_n = \frac{M_w}{P_{di}} \qquad (3)$$

where P_{di} is polydispersity index.

PA11 is a polycondensate therefore its polydispersity index shall be close to 2.[14] Previous studies reported no significant polydispersity change on degraded samples.[7]

Differential Scanning Calorimetry. DSC analyses were performed on a Perkin–Elmer Pyris Dynamic DSC with nitrogen as purge gas. Approximately 6 mg was weighed (±0.001 mg) and placed in Al-pans. The samples were analyzed with the following program:

1. Hold 30°C for 5 min
2. Heat 10°C/min to 225°C
3. Hold temperature for 5 min
4. Cool 10°C/min to 30°C
5. Hold temperature for 5 min
6. Heat 10°C/min to 225°C

Degree of Crystallinity Measurement. Crystallinity changes in aged samples were determined with DSC analysis using the following formula[15]:

$$\chi = \frac{dH_{\text{melt, polymer}} / dH_{\text{melt, crystal}}}{m_{\text{vacuum,200°C}}} \qquad (4)$$

where χ is a degree of crystallinity, $dH_{\text{melt, polymer}}$ is the melting enthalpy of the studied polymer, $dH_{\text{melt, crystal}}$ is the melting enthalpy for pure crystalline phase, and $m_{\text{vacuum,200°C}}$ is the 1—extractables (water and plasticizer) ratio as measured after 90 min at 200°C in a vacuum oven.

In addition to the standard method reported in literature[8,15,16] additive (plasticizer) extraction was also included in eq. (4) to ensure that the heat of melting is related to the actual mass of the polymer. The present study followed approximation used in El-Mazry's work.[8] It was assumed that the secondary lamellae possess the physical and thermal characteristics of the initial primary lamellae. Enthalpy was taken as an average of values obtained after first and second heating run.

Tensile Test

Measurements of stress vs. strain curves were made with a Schenk 10kN tensile-testing machine. The samples were 0.5 mm thick dumbbells shaped according to ISO 527 1BA. The tests started with a prestrain from a load of 3 N to avoid bias from strain in clamps or other parts of the instrument upon loading. The samples were stretched with a displacement rate of 2 mm/min until fracture or reaching 50% strain.

Choice of Tensile Properties. Stress–strain curves were obtained from the load displacement measurements. Stresses were calculated based on the initial cross-section of the samples in the thin part of the dumbbell specimens. Strains were calculated from the original length of the samples and machine displacement. This approach is not ideal, but the relative change between samples of different aging can be obtained fairly well. Two parameters from the stress–strain curves were evaluated: The Young's modulus and the tensile strength. The Young's modulus was derived from the slope between 0.2% and 0.5% strain of the stress–strain curves according to common practice in polymer science. This relatively broad measurement range should account well for the nonlinearity of the material. In addition, the tangential modulus was measured as the local slope of the stress–strain curve for different strain levels. The tensile strength was calculated by dividing the maximum load in each stress–strain curve by the original cross-sectional areas. True stress would be better for necked samples, but equipment to measure it in such small specimens was not available.

Dynamic Mechanical Thermal Analysis

Saturated Samples. The dynamic mechanical properties in flexure at the various stages in the aging process were measured by DMTA in a Rheometrics Solids Analyzer RSA II. Sample bars with dimensions 0.5 mm × 6 mm × 50 mm were tested in a dual cantilever beam arrangement. The tests were run with 0.2% strain at a frequency of 1 Hz and a temperature sweep from 25°C to 125°C. The temperature steps were 4°C and the soak time for each step was 120 s. The storage and loss modulus as well as tan δ were logged. Three samples were analyzed for each withdrawal.

Dry Samples. It was revealed that the thin sheet samples lost a considerable amount of moisture during the relative short time it took to perform the mechanical tests. Therefore, after aging in water at 120°C samples were left drying for 48 h in desiccator to ensure consistent conditions of the samples during testing. All dried samples used for DMTA testing were aged more than 7 days to make sure that effects of plasticizer extraction were minimized.

RESULTS AND DISCUSSION

The results for density, weight loss, plasticizer extraction, molecular weight, tensile test, and DMTA are presented below. Note that the weight loss, density, TGA and initial DMTA test were performed on water saturated samples, while the tensile and rheological tests, as well as second DMTA test were run on dry conditioned samples. The purpose of the study was to investigate the link between changes in the mechanical properties and morphology of PA11 as the material degraded.
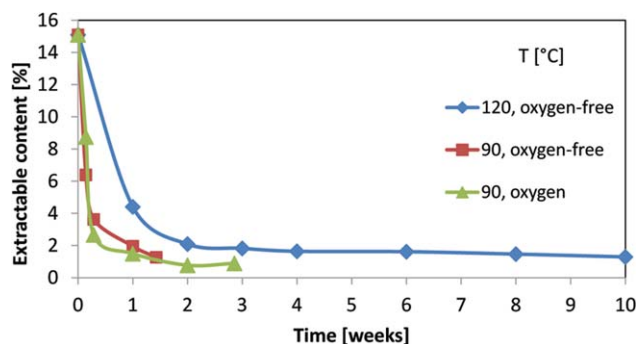
Figure 1. Plasticizer content for samples aged in 90°C and 120°C in both regular (TGA analyzed) and oxygen-free environment (vacuum oven analyzed). [Color figure can be viewed in the online issue, which is available at wileyonlinelibrary.com.]

Structure Characterization

Plasticizer Extraction and Water Saturation. Plasticizer is designed to soften the material, thus its depletion has a stiffening effect. Water is known to act in similar way to plasticizer, thus its absorption should have a softening effect.[17]

Volatile content analysis was performed for samples aged in 90°C and 120°C in both oxygen-free (vacuum oven/gravimetric analyzed) and oxygen-containing (TGA analyzed) environment. Figure 1 features the plasticizer extraction.

It can be seen that the rate of extraction is higher and residual plasticizer content lower for exposure at lower temperature. From purely kinetic point of view the opposite should be true, however above 95°C crystalline phase transitions occur in PA11 and crystallites gradually change from triclinic α to different hexagonal (γ, δ, and δ') forms.[18] This structural change may be instrumental for plasticizer extraction behavior.

At 90°C most of the plasticizer is depleted during the first two days of exposure. After about 2 weeks for both temperatures extractable content stabilizes and amounts to just under 2% at 120°C and 1% at 90°C. From that point further property changes can be mainly ascribed to morphological changes. Oxygen does not seem to contribute significantly to the extraction rate.

Water content remaining in samples after each exposure time is featured in Figure 2. Values here are very low compared to the saturation level of 3% as stated in Rilsan documentation.[3] The reason for this discrepancy is most likely water desorption from the samples while they have been stored and transported after exposures.[17] Such situation occurs also in dry conditioned samples making the effect of water content on mechanical properties negligible. In order to asses this effect for saturated samples the water uptake curve has been estimated from TGA water loss and reported desorption levels. The exact procedure is described in the technical appendix— Supporting Information eqs. (S1) and (S2) and its result is featured in Figure 3.

The analysis indicates the presence of large initial moisture content. Observed postsaturation water content drop ($\approx 0.5\%$) is described in the literature and associated with the extraction of additives from soluble materials present in the matrix.[17]
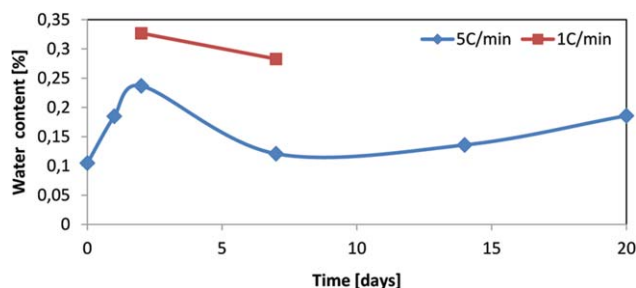
Figure 2. Water mass loss as measured with TGA at two heating rates for samples aged in 90°C. [Color figure can be viewed in the online issue, which is available at wileyonlinelibrary.com.]

Molecular Weight Evolution. Hydrolysis causes chain scissions contributing to lowering molecular weight and softening of the amorphous phase as well as its embrittlement.

Figure 4 features the comparison between measured number-average molecular weight and Jacques model predictions for exposures in 90°C and 120°C in oxygen-free water. CIV of the reference sample has been measured as 1.97 dL/g, which is equivalent to the number-average molecular weight of 40.64 kg/mol. For 90°, the prediction is fairly good for the first week of exposure. The result for 10 days is somewhat off, but it must be kept in mind that this data consist of single measurements only. The prediction for 120° is very good both regarding hydrolysis rate and position of equilibrium ($M_n = 17.33$ kg/mol or about 1.2 dL/g).

In addition some samples were also exposed to oxygen-containing water for 20 days. They showed no visible level of discoloration indicating only minor effects of parallel chain-scission mechanism of oxidation.

Crystallinity Ratio. Chain scissions destroy the entanglement network in the amorphous phase and liberate small molecular segments which can rearrange locally and initiate chemicrystalli-zation.[8] Crystallites contribute to stiffening of the material.

Crystallinity changes in aged samples were determined with DSC analysis. The degree of crystallinity was 21.7% for the reference sample. Since DSC tests were performed only on samples
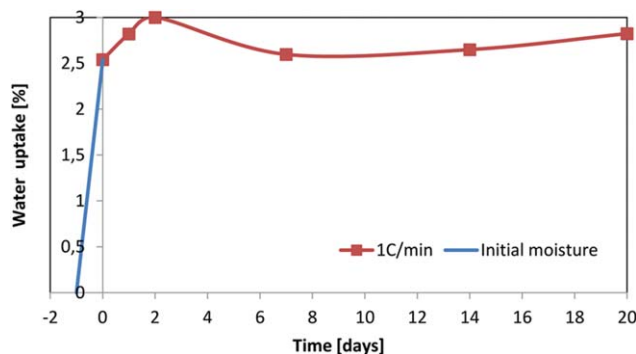
Figure 3. Water uptake estimate during aging in 90°C. It was obtained from measured water loss after accounting for desorption. [Color figure can be viewed in the online issue, which is available at wileyonlinelibrary.com.]
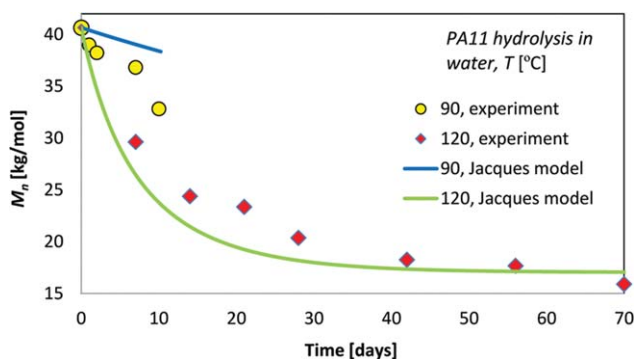
Figure 4. Experimental molecular weight evolution for samples aged in 90°C and 120°C and its prediction with Jacques model. [Color figure can be viewed in the online issue, which is available at wileyonlinelibrary.com.]

aged up to about 2 weeks, a different procedure was used to track crystallinity up to 10 weeks of exposure.

Crystallinity changes in samples aged more than 2 weeks (plasticizer effect minimized) were determined from density measurements. Densities of crystalline and amorphous phase were found to be 1.25 g/cm³ and 0.95 g/cm³, respectively, as calculated from eq. (5). Both were established from experimental sample density after 2 weeks and crystallinity χ at the same time from DSC analysis (at a slightly different exposure mode though).

A simple mixing rule for the density of the composite was utilized:

$$\varphi_{2w} = \varphi_c * \chi_{2w} * \varphi_a(1 - \chi_{2w}); \varphi_c > \varphi_a \quad (5)$$

where φ_{2w} and χ_{2w} are experimental sample density and crystallinity after 2 weeks of aging, respectively; φ_c, φ_a are fitted values for crystalline and amorphous density (assumed constant). Finally the degree of crystallinity as a function of time was calculated from the density evolution:

$$\chi(t) = \frac{\varphi(t) - \varphi_a}{\varphi_c - \varphi_a} \quad (6)$$

Each point is an average of three parallels.

Figure 5 shows the crystallinity changes as measured with both DSC and density measurements.

Property Characterization
Density Evolution. The curve obtained for the density as a function of time is shown in Figure 6. During the first 2 weeks of exposure plasticizer is being extracted resulting in an initial density drop. Then the density increases with the higher degree of crystallinity to finally stabilize on a plateau. The ultimate density is close to the initial one.

At all times the density remains higher than 1 g/cm³, therefore the material sinks in water.

CIV-Based Fracture Toughness. The CIV we obtained at equilibrium of long-term degradation is equivalent to the PA11 service acceptance criterion of 1.2 dL/g as in the API standard.[1] Therefore, samples aged for extended periods in high temperature water may risk undergoing ductile–brittle transition and
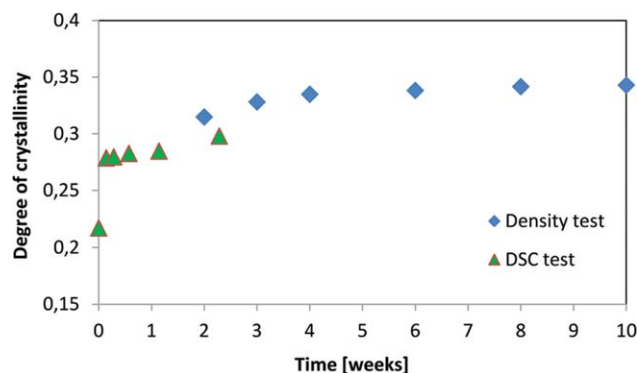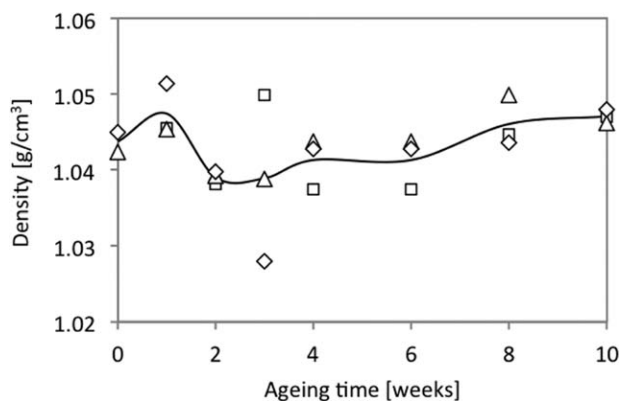
Figure 5. Crystallinity evolution of samples aged in 120°C as determined with DSC and density tests. [Color figure can be viewed in the online issue, which is available at wileyonlinelibrary.com.]

reduced elongation at break. However, at the same time CIV is far above the experience based failure criterion of 1.05 dL/g, so it is not certain whether embrittlement will happen.[1] The obtained CIV together with the industry experience indicate that elongation at break should still be greater than 200% and fracture toughness K_{IC} only marginally lower than 3 MPa m$^{1/2}$ in most cases of long-term hydrolytic degradation.[1,19] Therefore, occurrence of brittle failure must typically involve additional mechanisms of chain scission, e.g., oxidation or UV exposure.
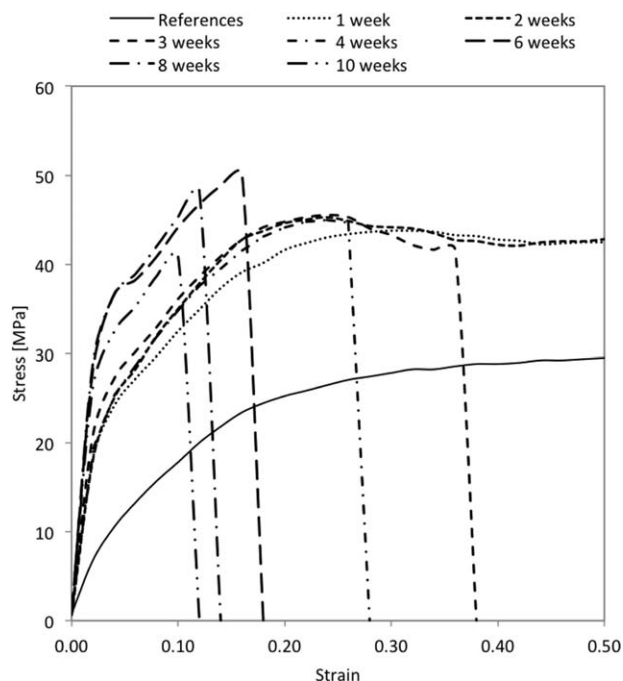
Tensile Test. From the stress–strain curves in Figure 7 it can be seen that the compliant behavior of the virgin reference material ceases already after 1 week of aging. In the same period of time the material shows a prominent increase in the secant modulus and tensile strength, as displayed in Figure 8.

The average secant modulus data indicate a sharp stiffness increase between forth and sixth week of exposure, nevertheless further Dynamic Mechanical Analysis ruled out that outcome.

The tangential modulus taken at different strain levels for samples aged 1 and 10 weeks is featured in Figure 9. This quantity provides more precise information of the mechanical behavior in case of polymers exhibiting nonlinear characteristic already at very low strains.[20]

Figure 7. Stress–strain plots for PA11 aged in water at 120°C for up to 10 weeks.

The large initial increase in mechanical strength and modulus was expected due to the rapid initial dissociation of plasticizer. On the other hand a reduction of strength and modulus was

Figure 8. Young's modulus (0.2–0.5%) and tensile strength of PA11 aged in water at 120°C. Error bars represent one standard deviation from parallel values for each exposure time. [Color figure can be viewed in the online issue, which is available at wileyonlinelibrary.com.]
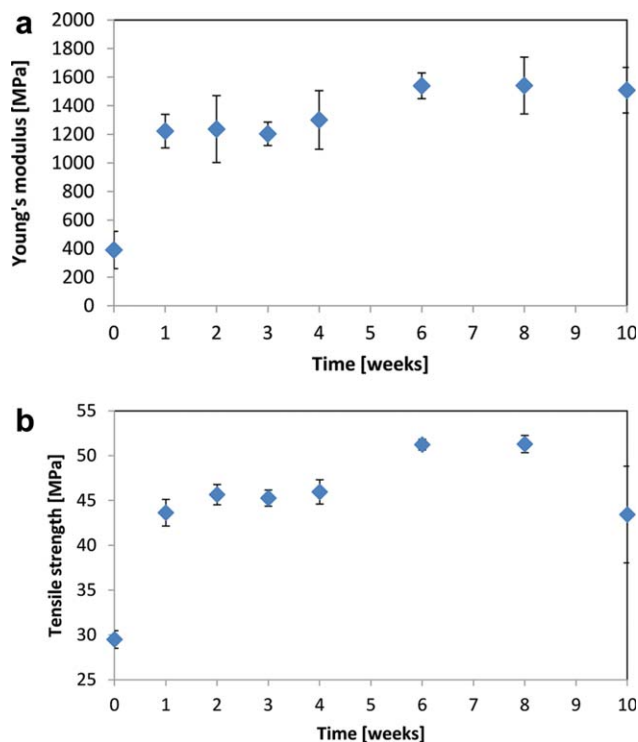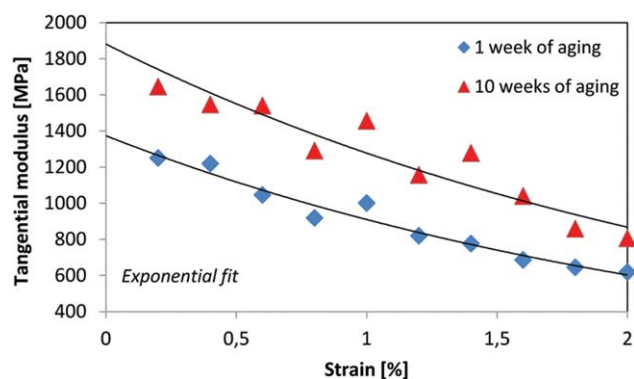
Figure 6. The density of PA11 during aging in water at 120°C. The different indicators represent the density of three individual samples and the line is the mean value at the given aging time.

Figure 9. Tensile tangential modulus at different strain levels for 1 and 10 weeks exposures. [Color figure can be viewed in the online issue, which is available at wileyonlinelibrary.com.]

also expected from the big initial decrease in molecular weight as in Figure 5. This reduction was not observed. Apparently, the increase in mechanical properties due to reduced plasticizer content hid the possible decrease in properties caused by reduced molecular weight.

Dynamic Mechanical Thermal Analysis. The stiffness of the material is represented by its complex modulus as calculated with the formula:

$$E^* = \sqrt{(E^{\mathrm{I}})^2 + (E^{\mathrm{II}})^2} \qquad (7)$$

where E^{I} is the storage modulus and E^{II} is the loss modulus.

Damping efficiency is represented by loss tangent as calculated with the formula:

$$\tan \delta = \frac{E^{\mathrm{II}}}{E^{\mathrm{I}}} \qquad (8)$$

Temperature dependence of dynamic mechanical properties. Figures 10 and 11 feature storage modulus and loss tangent of samples at different stages in degradation as a function of temperature. For all aging times the storage modulus decreases monotonically with temperature, while the loss modulus and loss tangent first reach a maximum. The peak value of tan δ curve marks the glass transition temperature of the material.

Aging time dependence of dynamic mechanical properties. In general stiffness (represented here by storage modulus since effect of loss modulus is negligible) increases with aging time for all temperatures. This involves a better ability to store energy during deformation.

Dry samples aged for 4 and 6 weeks deviate from this rule, but it was found that they contained one strongly aberrant withdrawal each, making this data questionable.

At room temperature the storage modulus of the saturated samples increased with almost 200% during the first 2 weeks, largely because of plasticizer depletion. The increase rate declined for longer aging times.
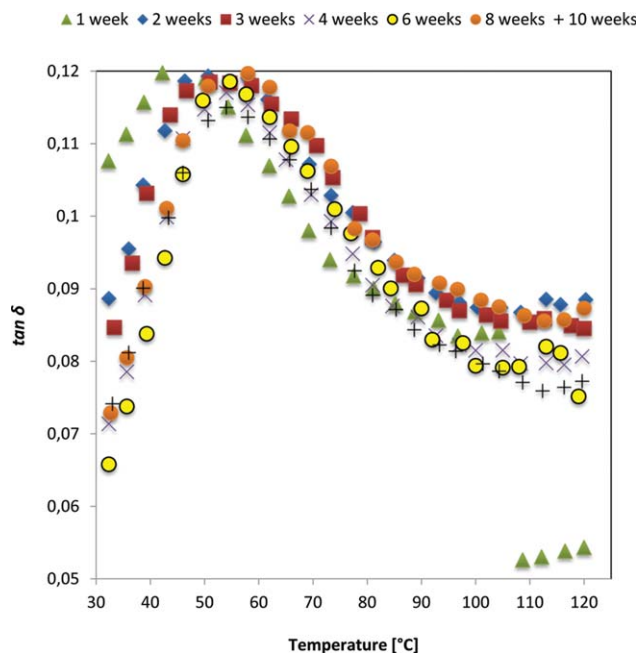
The development of the storage modulus for saturated samples at room temperature as a function of aging time is shown in
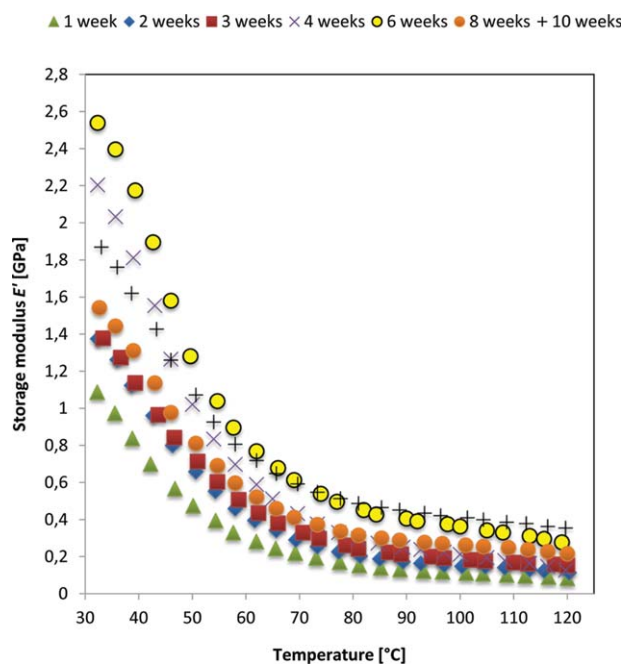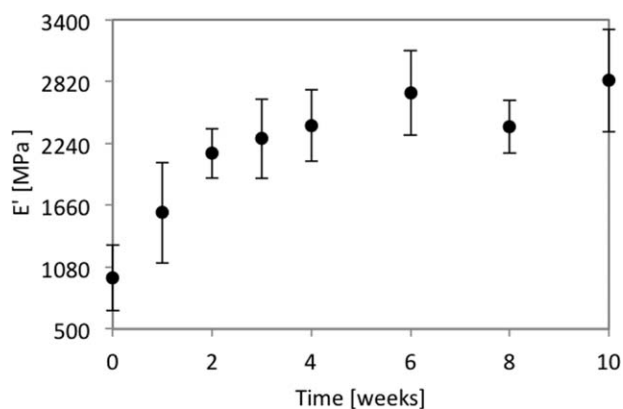

Figure 10. Storage modulus with temperature of PA11 samples aged in 120°C for 1–10 weeks and dry conditioned subsequently. [Color figure can be viewed in the online issue, which is available at wileyonlinelibrary.com.]

Figure 12. The trend was reproduced for higher temperatures, but the shifts were less remarkable.

Figure 13 features the storage modulus change with aging time at 30°C with error bars as well as mere averages for some other temperatures (this data showed much less variation).


Figure 11. Loss tangent with temperature of PA11 samples aged in 120°C for 1–10 weeks and dry conditioned subsequently. [Color figure can be viewed in the online issue, which is available at wileyonlinelibrary.com.]

Figure 12. Storage modulus for saturated samples at room temperature as a function of aging time.

The experimental data was statistically corrected by removing some outliers with the procedure described in the technical appendix (Supporting Information Fig. S1.)

It is clear, that for higher temperatures (as well as for previously tested dry samples) the modulus increases with time to finally settle down on a plateau region. It can be similarly interpreted for 30°C as indicated by the trendline. This change in modulus with time confirms the validity of competing mechanisms: degradation creating low MW species decreasing the modulus and crystallization of low MW species increasing the modulus. It also largely rules out the occurrence of a previously considered sharp modulus increase after 4 weeks of exposure. A similar trend with aging time and temperature was observed for the loss modulus. Damping efficiency (represented by the loss tangent) seems to be affected negatively by the degradation for
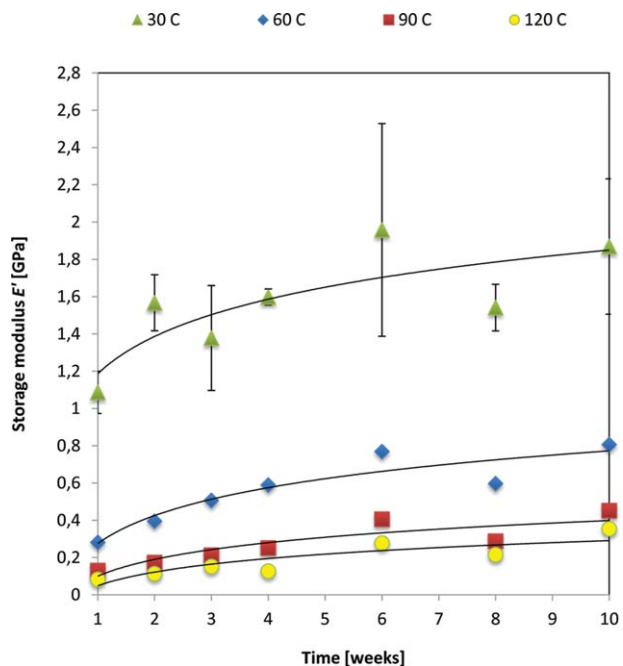
Figure 13. Storage modulus for dry samples at different temperatures as a function of aging time. [Color figure can be viewed in the online issue, which is available at wileyonlinelibrary.com.]
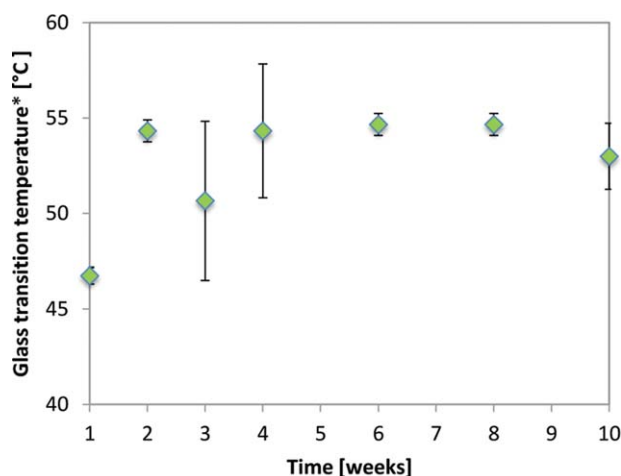
*Estimated from maximum point of tan δ curve at 1 Hz

Figure 14. Glass transition temperature for dry samples as a function of aging time. Error bars represent one standard deviation. [Color figure can be viewed in the online issue, which is available at wileyonlinelibrary.com.]

samples in the glassy state. The reduction of loss tangent was however not reproduced after samples have reached the glass transition temperature.

Aging time dependence of glass transition temperature. Modulus shifts along the temperature axis imply that the glass transition temperature T_g increases as the material ages. DMTA allows estimating the glass transition temperature as a function of time as shown in Figure 14. It can be clearly seen, that the glass transition temperature first rapidly increases and then after 2 weeks reaches a plateau region. T_g in this region ranges between 51°C and 55°C.

According to Fox and Flory[21] the T_g of amorphous phase should decrease as the degradation proceeded and the molecular weight decreased. However, if the lower molecular weight products from the chain scission do not diffuse out of the material structure, but distribute in the polymer matrix, they will reorganize and cause a higher degree of crystallinity.[8]

A possible explanation and hypothesis in the present study is the T_g increase caused by immobile crystallites constraining amorphous chain segments, which now need higher energy input to get mobility levels of rubbery state. A previous study on aging of PA11 established the presence of lower molecular weight products in the polymer matrix by DSC measurements and the present study already confirmed the increase in crystallinity with aging time.[9]

Comparison between saturated and dried samples. Saturated samples are routinely stiffer than dried ones, which seems to be contrary to previous experience and theory. It means that either some important effects have been overlooked or more likely, that the DMTA apparatus has produced unknown sort of systematic error.

Figure 15 features a similar comparison with regard to glass transition temperature. It can be concluded, that the presence of water decreases the glass transition temperature. The plateau
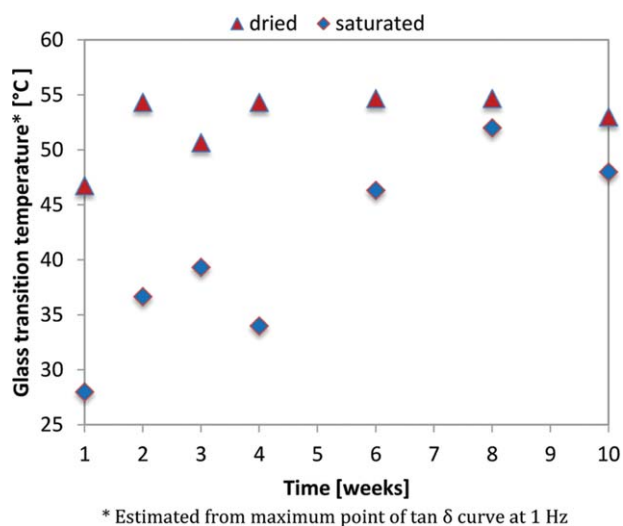
Figure 15. Glass transition temperature for dry and saturated samples as a function of aging time. [Color figure can be viewed in the online issue, which is available at wileyonlinelibrary.com.]

for saturated samples is reached much later in the degradation process, however it has similar value. This would indicate that water has been largely extracted by the eighth week of exposure.

Comparing Figures 11 and 16 allows concluding that saturation with water generally decreases damping efficiency of the PA11.

Property Evolution. Figure 17 features a general scheme of stiffness evolution with aging time for thin sheet PA11. After
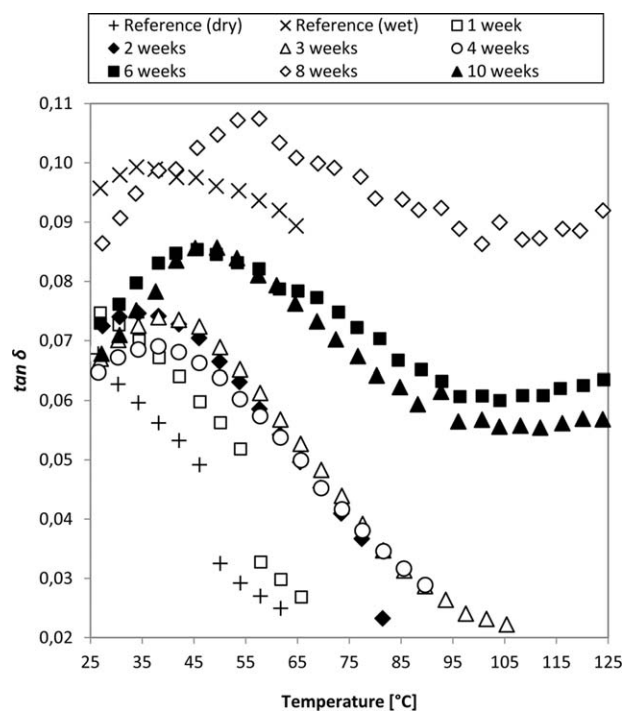
Figure 16. The tan δ in flexure for PA11 aged for different periods in deoxygenated water at 120°C. The analyses were performed on samples saturated with water. Each point in the scatter represents the mean of three samples.
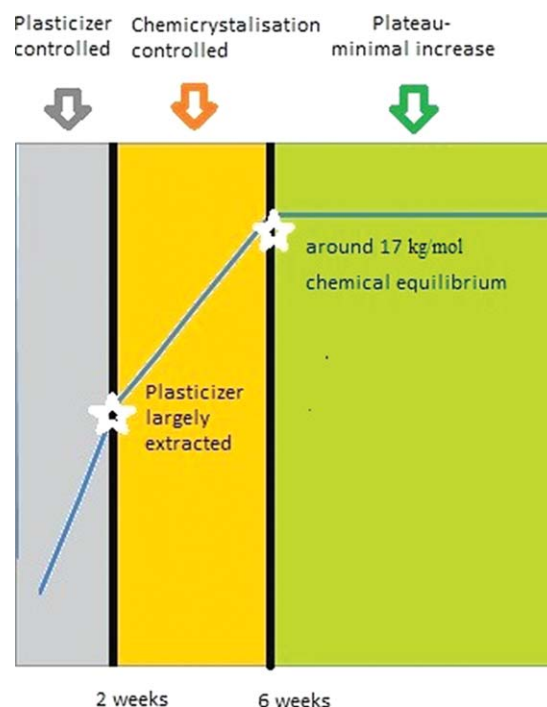
Figure 17. General scheme of PA11 stiffness evolution with aging time (thin sheet samples). [Color figure can be viewed in the online issue, which is available at wileyonlinelibrary.com.]

analyzing experimental data three distinct control domains have been identified:

1. *Plasticizer control.* With exception of the very initial period (first 1–2 days, sample getting saturated with water) stiffness increases following plasticizer extraction. Difference in modulus of over 1 GPa between plasticized and unplasticized PA11 grade is reported in the product specification.[3] Therefore, effects of plasticizer extraction dominate over 10% crystallinity increase in the early stage of degradation. Most of the plasticizer is already depleted after a few days and after 2 weeks effects of further extraction should be negligible.

2. *Chemicrystalization control.* Plasticizer extraction and water saturation already came to their full effect in the previous phase, leaving chain scission induced softening of the amorphous phase and crystallization of the lower molecular weight products as the two governing mechanisms for stiffness evolution. Experiments showed that for the following month the modulus continues to increase with lower pace indicating that the stiffening effect due to crystallinity increase dominates here over continuous softening of the amorphous phase. The magnitude of this domination diminishes with time as degradation and chemicrystalization slow down.

3. *Plateau region.* After about 6 weeks into exposure the molecular weight gets asymptotically close to 17 kg/mol—equilibrium between hydrolysis and repolymerization. The modulus will continue to increase at an infinitesimal level thus essentially staying constant—this is the limit of water induced degradation.

The change in the material structure in the aging periods based on stiffness evolution is shown in Table I. The mechanical and

Table I. PA11 Structural Parameters Evolution Dynamics with Aging Time

Aging time (weeks)	Plasticizer content	Crystallinity ratio	Molecular weight
0–2	↓	↑	↗
2–6	–	↙	↗
6–∞	–	–	–

volumetric properties can be expressed in an equivalent way, as shown in Table II. They can be seen as different functions of the three structural parameters from Table I. All these quantities are mutually interconnected thus it is possible to break their variability into similar time periods. This interconnection is strongly pronounced after 6 weeks of aging when all properties and structural parameters tend to reach a plateau.

Observing changes in the microstructure in detail, e.g., with an SEM, would provide parameters like crystallite size, shape, and orientation to supplement the information given by degree of crystallinity. Such studies should be performed in the future to improve the understanding of the underlying phenomena and the model predictions.

Thick samples. Based on the above it is also possible to estimate stiffness evolution of real life thick samples. Plasticizer molecules are relatively large and it would take a long time for them to diffuse out of a thick liner. Slow removal of the plasticizer would cause a slow gradual increase in modulus over the years. In short term this increase would not be significant. Since diffusion of water is very fast in polyamides[22] chemicrystalization would control stiffness increase for the first 6 weeks. Then the degree of crystallinity reaches plateau, but plasticizer continues to be slowly extracted. The modulus continues its slow gradual increase and is now controlled by plasticizer extraction. Therefore, for thick samples, stiffness plateau is reached after several years, once the plasticizer is completely diffused out.

CONCLUSIONS

There are four main mechanisms of property change. Plasticizer extraction contributes to stiffening of the material (modulus and strength increase), T_g increase and density decrease—partially diminished by water absorption acting as plasticizer. Moreover hydrolysis has a dualistic effect on properties: chain scissions destroy the entanglement network in the amorphous phase (softening, embrittlement, T_g decrease) and liberate small molecular segments which rearrange locally and initiate chemicrystalization (stiffening, T_g and density increase).

Table II. PA11 Property Evolution Dynamics with Aging Time

Aging time (weeks)	Modulus	Strength	T_g	Density
0–2	↑	↑	↑	↗
2–6	↙	↙	–	↙
6–∞	–	–	–	–

Experimental results regarding changes in morphology and properties of PA11 under hydrolytic degradation in 120°C have been compared and the main findings are listed as follows:

- Occurrence of brittle failure by hydrolysis only is rare and typically involves additional mechanisms of chain scission, e.g., oxidation or UV exposure
- Mechanical properties evolution can be divided into three control domains for thin PA11 materials:
  1. *Plasticizer control*—first 2 weeks, stiffness and strength—rapid increase
  2. *Chemicrystalization control*—following month, stiffness, and strength—moderate increase
  3. *Plateau region*—after about 6 weeks, stiffness, and strength—infinitesimal increase
- The glass transition temperature increases as the degradation proceeds—contrary to Fox and Flory theory for amorphous regions. It can be explained by the fact, that amorphous chain segments get constrained by the immobile crystallites following chemicrystalization

Moreover interesting supporting findings have been listed below:

- PA11 sinks in water at all aging times. The ultimate density is close to the initial one
- Damping efficiency (loss tangent) is affected negatively by degradation for samples in the glassy state, but not in rubbery state
- Presence of water contributes to the decrease in both glass transition temperature and damping efficiency

This work investigated the link between mechanical behavior and morphology of PA11 during degradation through tensile testing, DMTA and material characterization techniques. Experimental results obtained here will be compared with a multiscale model for PA11 hydrolytic degradation in another article (Part 2). Fatigue behavior and some additional analysis should also be detailed elsewhere.

ACKNOWLEDGMENTS

REFERENCES

1. API TECHNICAL REPORT 17TR2, The Ageing of PA 11 in Flexible Pipes, API Publishing Services: Washington, DC, **2003**.
2. API RECOMMENDED PRACTICE 17B, Recommended Practice for Flexible Pipe, API Publishing Services: Washington, DC, **2008**.
3. Rilsan® PA11: Created From a Renewable Source; Arkema: France, **2012**.
4. Boschee, P. *Oil Gas Facil.* **2012**, *15*.
5. Groves, S. Ed. 20th International Conference on Offshore Mechanics and Arctic Engineering, Rio de Janeiro, Brazil, ASME: **2001**.

6. Meyer, A.; Jones, N.; Lin, Y.; Kranbuehl, D. *Macromolecules* **2002**, *35*, 2784.

7. Jacques, B.; Werth, M.; Merdas, I.; Thominette, F.; Verdu, J. *Polymer* **2002**, *43*, 6439.

8. El-Mazry, C.; Correc, O.; Colin, X. *Polym. Degrad. Stab.* **2012**, *97*, 1049.

9. Romao, W.; Castro, E. V. R.; Filho, E. A. S.; Guimaraes, R. C. L.; Silva, A. L. N.; Teixeira, S. C. S. *J. Appl. Polym. Sci.* **2009**, *114*, 1777.

10. Domingos, E.; Pereira, T. M. C.; Castro, E. V. R.; Guimaraes, R. C. L.; Romao, W. *X-Ray Spectrom.* **2013**, *42*, 79.

11. Pinel, E.; Mason, J.; O'Brien, G. NACE International Meeting, Corrosion Proceedings—Paper #04713, March, New Orleans, USA, **2004**.

12. Mazan, T.; Berggren, R.; Jørgensen, J. K.; Echtermeyer, A. T. *J. Appl. Polym. Sci.* to be submitted for publication.

13. ASTM D792-08, Standard Test Methods for Density and Specific Gravity (Relative Density) of Plastics by Displacement, ASTM, USA, **2008**.

14. Schnabel, W. Aspects of Degradation and Stabilisation of Polymers; Elsevier: Amsterdam, **1978**; Chapter 4, p 149.

15. Sichina, W. J. DSC as Problem Solving Tool: Measurement of Percent Crystallinity of Thermoplastics. PETech-40 Thermal Analysis, PerkinElmer, **2000**.

16. Ying, S.; Lin, Y.; Tao, Y. *J. Appl. Polym. Sci.* **2008**, *110*, 945.

17. Silva, L.; Tognana, S.; Salgueiro, W. *Polym. Test.* **2013**, *32*, 158.

18. Zhu, J.; Zhang, X. Y.; He, B. 12th International Symposium on Electrets, September 11–14, Bahia, Brazil, **2005**.

19. Berger, J. The Compatibility and Aging of Polyamides With Production Fluids. EVONIK industries, MERL Oilfield Engineering With Polymers Conference, October 23–25, London, UK, **2012**.

20. Echtermeyer, A. T. Proceedings of 2nd European Conference on Composites Testing & Standarisation, September 13–15, Hamburg, Germany, **1994**.

21. Fox, T. G.; Flory, P. J. *J. Appl. Phys.* **1950**, *21*, 581.

22. Wu, P.; Siesler, H. W. *Chem. Mater.* **2003**, *15*, 2752.